Online Supplement

Method

Clinical Recordings and Data Reduction

Unipolar electrograms were acquired using a noncontact mapping catheter (EnSite 3000; Endocardial Solutions, Inc., St. Paul, MN, USA). The EnSite 3000 system incorporates a multielectrode array (MEA) catheter, amplifier, and workstation[1-2]. The MEA consists of 64 wires attached to laser-etched electrodes and mounted on a 7.5-mL balloon. In the present study, 70% of all measurements were <35mm from the center of the MEA and 90% were <45mm. Although minor inaccuracies in electrogram reconstruction occur with MEA to endocardium distances of >34mm, this error remains small with distances up to 50mm from the center of the array[1]. MEA electrical signals are amplified, sampled at 1.2 kHz, and filtered with a 0.1-300Hz passband[1-2]. From each pacing study, a subset of 256 virtual unipolar electrograms were exported as an ASCII data file for analysis and mapping. The 256 multichannel recordings were obtained as sixteen virtual electrogram sites separated by 11.25º of latitude along each of sixteen lines of longitude separated by 22.5º. The average distance between adjacent virtual recoding sites on the heart surface was approximately 5mm although the spacing varied according to the shape of the heart and the polar coordinate location of the sites. Following data analysis, the map3d computer program[3] was used to display each map point on a three-dimensional computerized grid according to its Cartesian coordinates.

Mapping activation in VT

For our retrospective clinical data analysis, VT events were subdivided into nonsustained (duration from onset to spontaneous termination <30s) and sustained (duration >30s). The VT cycle lengths were measured from the R-R interval of the electrocardiogram. To construct isochronal activation maps, custom-designed computer software was used to manually mark the intrinsic deflection of each unipolar electrogram at the point of sharpest slope, or at the approximate center point when multiple intrinsic deflections with sharp slopes were present[4]. Activation times referenced to the onset of the arbitrary time window of a representative cycle of VT were plotted on the computerized map grid, isochrones were set at 20-50ms intervals, and arcs of conduction block were overlaid where wavefronts on opposite sides of the arcs moved in different directions[4].

Analysis of Sinus Rhythm Activation

All sinus rhythm recordings used for quantitative analysis were obtained without pacing the heart. The method for analyzing multichannel recordings obtained during sinus rhythm is illustrated in Figure S1. Panels A-B show the noncontact endocardial activation map of a selected patient during sinus rhythm (256 virtual sites in total) with anatomical locations noted. For clarity, activation times are only shown for a subset of all sites. Two large (i.e., >2 x 2cm)[4-6] centers of late activation where reentry can potentially form are evident on the posterior endocardial surface (panel B: sites with encircled activation times). From each area of latest activation, arrows are drawn toward areas of earlier activation so that 4-7 recording sites on the computerized electrode grid reside adjacent to each arrow[4,6]. For any particular arrow, if only three successive sites in the same direction have activation times which progressively decrease, the arrow is drawn but it is extended

to the nearest additional site in the same direction (four sites in all). If more than seven successive sites along the same direction have progressively decreasing activation time, the arrow is truncated at the seventh site. The arrows so formed are located in regions denoted by gray shading (Figure S1B).

The linear regression of activation times along each arrow is computed. An example of the computation is provided for the solid arrow that is overlapped on the map grid. Activation times for recording sites residing adjacent to it are 84, 77, 46, 17, and 5ms. The regression coefficient r^2 = 0.97 and the slope = 21.8ms. The average distance between the 256 virtual recording sites is ~5mm, therefore the activation gradient (AG) along this arrow is 0.23mm/ms. The activation gradient corresponds to the conduction velocity along the arrow if the activation wavefront is moving in the same direction as the arrow is pointing, which is usually the case. The regression analysis for all arrows is shown in Table S1. The basal region had slower mean activation gradient according to the slope of the regression line (0.34mm/ms) and a more uniform progression of activation times according to r^2 (0.89) and p (0.01). Since this region has relatively uniform slow conduction (USC), it was selected as being the most likely location at which an isthmus that is the source of ventricular tachycardia will form, in accord with a previous canine postinfarction study[6]. The regression line with both the slowest AG and largest r^2 as optimized from a two-dimensional scatterplot of r^2 versus p value is outlined in bold in Table S1 and it corresponds to the regression computed for the solid arrow on the map. This arrow is called the primary path, which is anticipated to approximately

overlap the location where the isthmus of the reentrant circuit will form during ventricular tachycardia[6].

The algorithm used to delineate the reentry isthmus boundaries using the virtual noncontact unipolar recordings of activation time is similar to that which is used for analysis of the bipolar electrogram duration[6]. Locations within the USC region at which the difference in sinus rhythm activation time between any 2 adjacent sites was ≥15 ms were marked on the computerized map grid. Selected nodes were then connected to form the border of a contiguous region based on the following algorithm: (1) the region must overlap >50% of the primary path; (2) nodes were connected so as to (a) minimize the maximum distance between connections, followed by (b) minimization of the mean distance between connections; and (3) the inscribed region must have surface area ≥2.0 cm^2 (the approximate minimum isthmus surface area that was observed). The polygon so formed is the estimated isthmus, shown in Figure S1C as a thin solid line, with the nodes denoted by solid circles. Locations where functional block lines would be expected to form during reentry were drawn as thick black lines along segments of the polygon with ≥15 ms sinus rhythm activation time between the recording sites. The activation times at adjacent sites along the primary path can differ by > 15ms during sinus rhythm because conduction is uniform and slow. During reentrant tachycardia, such areas often form part of the isthmus boundary.

Discussion

Isthmus Characteristics

The results of our retrospective study compliment that of another clinical study of patients with structural heart disease[7], in which the VT origin was a macroreentrant circuit having one or two loops rotating about functional or anatomical conduction barriers, and in which the same reentry isthmus was shared by 2-4 circuit morphologies, with differences in entrance and exit point locations being the distinguishing factor between morphologies[7]. The average isthmus dimension in these patients was 3.1cm x 1.6cm[7] whereas in our patient series it was 10.1cm^2 (~3.1cm x 3.1cm square) for sustained and 4.8cm^2 (~2.2cm x 2.2cm square) for transient reentrant tachycardia (Table 2 in the manuscript). Hence, when complete endocardial reentrant circuits are mappable in human postinfarction patients, similar characteristics of isthmus size and changes in entrance and exit point location at a stationary isthmus perimeter, pertaining to changes in circuit morphology, can be observed and measured. The relationships of the isthmus perimeter to reentry duration and form that we found are also similar to those demonstrated in a canine postinfarction study of two-dimensional circuits forming in the epicardial border zone[5]. Since a single ablation lesion at an entrance or exit point to the reentry isthmus can prevent reinduction of multiple reentrant circuit morphologies in canine infarct border zone[8], prevention of reinduction of multiple clinical reentrant circuit morphologies with a single lesion may be possible using sinus rhythm map-guided catheter ablation. By predicting from sinus rhythm analysis the precise location and boundaries of the USC region at which a reentrant circuit is most likely to form, it may be possible to perform targeted ablation that will prevent reentrant tachycardia that may

originate from a particular region of the heart, both existing and preventatively. The value of sinus rhythm map-guided catheter ablation also stems from the fact that it provides a complete map of the endocardial substrate so that lesions can be placed to minimize the possibility that new or modified reentrant circuits will occur from the anatomical block lines that are produced. This may reduce medium/long term ventricular tachycardia recurrences and the need for follow-up, a subject of future study.

Comparison to Other Mapping Methods

In patients with structural heart disease, entrainment mapping remains the gold standard for defining the protected isthmus and other components of the VT circuit, yet successful ablation of reentry is achieved in only 60-90% of cases[9]. Frequent recurrences of VT despite implantable cardioverter-defibrillator (ICD) and antiarrhythmic drug therapy are a typical indication for catheter ablation[10]. The sinus rhythm analyses already developed by other clinical investigators have met with some success for improving reentrant VT ablation accuracy in post-MI patients, but have largely been empirically guided by non-specific features such as low-voltage regions, electrically unexcitable scar, and localization of late sinus rhythm electrogram components[11].

In Figures 1-4 in the manuscript, sinus rhythm activation is late within or near the isthmus location in accord with previous clinical[1,4,11] and canine[5-6,8] investigations of postinfarction reentrant ventricular tachycardia. Late sinus rhythm activation at the isthmus is probably associated with the presence of the thinnest border zone which has been observed to occur at these areas[12-14]. Since tissue resistivity is anticipated to increase

in proximity to the infarct[13,15], wavefront propagation would be expected to be slowed at the isthmus location during sinus rhythm, causing delayed activation there. In patients with infarct-related VT, noncontact map-guided ablation is associated with a high acute success rate, yet only 42.5% of patients remain free from VT/VF three years after ablation[16]. The extent and complexity of the scar-related arrhythmic substrate and potential for reentrant circuits likely contributes to the difficulty in achieving permanent freedom from tachycardia[17].

Sinus rhythm mapping can potentially improve outcome, particularly in cases where induced tachycardia is poorly tolerated or non-sustained, and can possibly be used to identify the regions of activation complexity that have characteristic properties, precisely identifying them as arrhythmogenic[18]. By our technique, better understanding and characterization of activation in sinus rhythm has revealed features that correlate specifically with the location of the reentrant circuit. This would be expected to be of benefit in both targeting ablation and to identify the target arrhythmogenic regions of the infarcted ventricle based on these criteria. Such left ventricular activation patterns may even identify and provide primary prevention in patients at risk of post-infarction reentry.

Several pacing and voltage mapping studies have described bystander areas (blind alleys or cul-de-sacs) which are not part of the actual reentry isthmus but have similar properties[11,17-18]. We believe these areas are potential substrates for reentry even though they do not participate in reentrant circuits that can be provoked during clinical study. Previous work has shown that multiple reentry morphologies often share a common

isthmus location, and differ only in the exact path and the entrance and exit points[8,19]. In some instances, distinct substrates are responsible for differing reentry morphologies[19]. The method that we describe herein selects the most likely isthmus location (i.e. the estimated isthmus boundary) and the direction of propagation during the diastolic interval of reentrant ventricular tachycardia (primary path) based on regression analysis. Other propagation directions (arrows of decreasing activation time, Figure S1 and Figures 1-2 in the manuscript) and other potential isthmus locations (late activation area at Apex, Figure S1) are possible and may correspond to bystander areas which are less likely to cause a particular clinical reentrant ventricular tachycardia morphology. Thus while our analysis does not directly differentiate isthmus from bystander regions, we believe that the bystander regions during one particular reentry morphology may be part of the circuit during other reentry morphologies[8,19].

Recently, Magnetic Resonance Imaging (MRI) has been used in canine postinfarction to measure changes in infarct border zone geometry for calculation of wavefront curvature[14]. Based on the methodology, functional block lines present during reentrant ventricular tachycardia were predicted to coincide with locations of abrupt increase from thinnest to thicker border zone tissue. As in canine postinfarction, sinus rhythm discontinuities and reentrant ventricular tachycardia characteristics in clinical postinfarction are likely affected by infarct border zone geometry[14], as well as changes in gap-junctional connections between myocytes[13], the subject of future study.

Conclusions

Analysis of noncontact activation maps acquired during normal sinus rhythm are useful to define the location and shape of the reentry isthmus that will occur during ventricular tachycardia in post-MI patients. The estimated isthmus boundary was derived from differences ≥15ms in sinus rhythm activation time at neighboring sites and was in agreement with the actual isthmus boundary during reentry. The estimated direction of propagation during the diastolic interval of reentry was delineated by the primary path and was in accord with the actual propagation direction. The algorithm used for estimating isthmus location, its boundaries, and propagation direction during the diastolic interval was essentially the same as that used previously for bipolar canine postinfarction recordings[6]. Additionally it was shown that nonsustained reentry tends to occur when isthmus size is relatively small and border discontinuities are large as described previously[5]. Although the location where ablation lesions should be positioned to stop reentrant ventricular tachycardia may be estimated from sinus rhythm analysis, prospective clinical evaluation will be necessary for evaluation.

Table 2: Regression Analysis

Arrow	AG - BASE	r^2	p	AG - APEX	r^2	p
1	0.49	0.728	0.0310	0.81	0.584	0.2360
2	0.53	0.768	0.0220	0.46	0.909	0.001
3	0.32	0.977	0.001	0.60	0.699	0.1640
4	0.30	0.917	0.003	0.48	0.742	0.1390
5	0.29	0.959	0.001	0.46	0.609	0.2200
6	**0.29**	**0.970**	**0.001**	0.31	0.814	0.0980
7	0.25	0.834	0.0300	0.59	0.492	0.2990
8	0.29	0.921	0.004	0.41	0.969	0.002
MN±SE	0.34±0.039	0.89±0.034	0.011±.005	0.52±0.053	0.73±0.058	0.144±0.038

AG = activation gradient

References

1. Schilling RJ, Davies DW, Peters NS. Characteristics of sinus rhythm electrograms at sites of ablation of ventricular tachycardia relative to all other sites: a noncontact mapping study of the entire left ventricle. J Cardiovasc Electrophysiol 1998;9:921–933.

2. Schilling RJ, Peters NS, Davies DW. Simultaneous endocardial mapping in the human left ventricle using a noncontact catheter: comparison of contact and reconstructed electrograms during sinus rhythm. Circulation. 1998;98:887–898.

3. MacLeod RS, Johnson CR. Map3d: Interactive scientific visualization for bioengineering data. IEEE Eng Med Biol Soc 15th Annual International Conference, pp30-31, IEEE Press, 1993.

4. Ciaccio EJ, Chow AW, Davies DW, Wit AL, Peters NS. Localization of the isthmus in reentrant circuits by analysis of electrograms derived from clinical non-contact mapping during sinus rhythm and ventricular tachycardia. J Cardiovasc Electrophysiol 2004;15:27-36.

5. Ciaccio, EJ. Ventricular tachycardia duration and form are associated with electrical discontinuities bounding the isthmus of the reentrant circuit. J Cardiovasc Electrophys 2005;16:646-654.

6. Ciaccio EJ, Tosti AC, Scheinman MM. Relationship between sinus rhythm activation and the reentrant ventricular tachycardia isthmus. Circulation 2001;104:613-619.

7. de Chillou C, Lacroix D, Klug D, Magnin-Poull I, Marquié C, Messier M, Andronache M, Kouakam C, Sadoul N, Chen J, Aliot E, Kacet S. Isthmus characteristics of reentrant ventricular tachycardia after myocardial infarction. Circulation 2002;105:726-731.

8. Ciaccio EJ, Coromilas J, Costeas CA, Wit AL. Sinus rhythm electrogram shape measurements are predictive of the origins and characteristics of multiple reentrant ventricular tachycardia morphologies. J Cardiovasc Electrophysiol 2004;15:1293-1301.

9. Dixit S, Callans DJ. Mapping for ventricular tachycardia. Cardiac Electrophysiology Review. 2002;6:436-441.

10. Strohmer B, Hwang C. Ablation of postinfarction ventricular tachycardia guided by isolated diastolic potentials. Europace 2003;5:375-380.

11. Stevenson WG. Catheter ablation of monomorphic ventricular tachycardia. Current Opinion Cardiol 2005;20:42-47.

12. Wit AL, Allessie MA, Bonke FI, Lammers W, Smeets J, Fenoglio JJ Jr. Electrophysiologic mapping to determine the mechanism of experimental ventricular tachycardia initiated by premature impulses. Am J Cardiol 1982;49:166-185.

13. Peters NS, Coromilas J, Severs NJ, Wit AL. Disturbed connexin43 gap junction distribution correlates with the location of reentrant circuits in the epicardial border zone of healing canine infarcts that cause ventricular tachycardia. Circulation 1997;95:988-996.

14. Ciaccio EJ, Ashikaga H, Kaba RA, Cervantes D, Hopenfeld B, Wit AL, Peters NS, McVeigh ER, Garan H, Coromilas J. Model of reentrant ventricular tachycardia based upon infarct border zone geometry predicts reentrant circuit features as determined by activation mapping. Heart Rhythm 2007;4:1034-1045.

15. Kléber AG and Rudy Y. Basic mechanisms of cardiac impulse propagation and associated arrhythmias. Physiol Rev 2004;84:431-488.

16. Segal OR, Chow AW, Markides V, Schilling RJ, Peters NS, Davies DW. Long-term results after ablation of infarct-related ventricular tachycardia. Heart Rhythm 2005;2:474-482.

17. Calkins H, Epstein A, Packer D, Arria AM, Hummel J, Gilligan DM, Trusso J, Carlson M, Luceri R, Kopelman H, Wilber D, Wharton JM, Stevenson W. Catheter ablation of ventricular tachycardia in patients with structural heart disease using cooled radiofrequency energy: results of a prospective multicenter study. Cooled RF Multi Center Investigators Group. Amer Coll Cardiol 2000;35:1905-1914.

18. Ellison KE. Stevenson WG. Sweeney MO. Lefroy DC. Delacretaz E. Friedman PL. Catheter ablation for hemodynamically unstable monomorphic ventricular tachycardia. J Cardiovasc Electrophysiol 2000;11:41-44.

19. Costeas C, Peters NS, Waldecker B, Ciaccio EJ, Wit AL, Coromilas J. Mechanisms causing sustained ventricular tachycardia with multiple QRS morphologies: results of mapping studies in the infarcted canine heart. Circulation 1997;96:3721-3731.

Figure Legends

S1. Details of the methodology to determine the reentry isthmus perimeter by sinus rhythm and ventricular tachycardia activation mapping. For all activation maps, activation times are referenced to the earliest time on the grid which was set to 1ms.

Fig S1

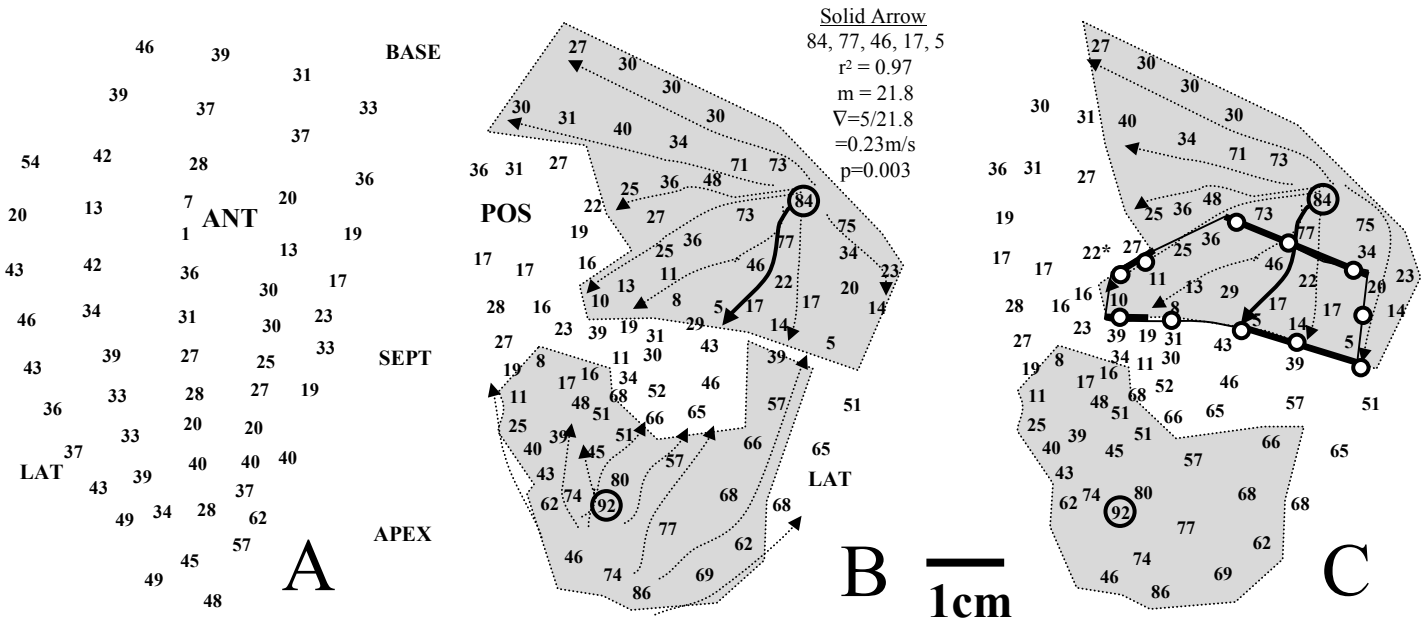
BASE
ANT
SEPT
LAT
APEX
A
POS
LAT
Solid Arrow
84, 77, 46, 17, 5
r² = 0.97
m = 21.8
∇=5/21.8
=0.23m/s
p=0.003
B
1cm
C